On the Parameter Extraction of a Five-Parameter Double-Diode Model of Photovoltaic Cells and Modules

Mohammad Hejri, Hossein Mokhtari, Mohammad Reza Azizian, Mehrdad Ghandhari, and Lennart Söder

***Abstract*—The main contribution of this paper is to present a new set of approximate analytical solutions for the parameters of a photovoltaic (PV) five-parameter double-diode model that can be used as initial values for the numerical solutions based on the Newton–Raphson method. The proposed formulations are developed based on only the limited information given by the PV manufacturers, i.e., the open-circuit voltage (V_{oc}), the short circuit current (I_{sc}), and the current and voltage at the maximum power point (I_m and V_m). Compared with the existing techniques that require the entire experimental *I–V* curve or additional information such as the slope of the *I–V* curves of the open circuit and the short circuit points, the proposed technique is quite independent of these additional data, and, it is therefore, a low cost and fast parameter extraction method. The accuracy of the theoretical *I–V* curves is evaluated through the comparison of the simulation results and experimental data. The results of the application of the proposed technique to different PV modules show the accuracy and validity of the proposed analytical-numerical method.**

***Index Terms*—Double-diode model, initial point, parameter identification, photovoltaic (PV), PV cells and modules.**

I. Introduction

Developing suitable models for photovoltaic (PV) cells and modules to simulate and predict their behavior is of particular importance for the design, manufacturing, and evaluation of PV systems. There are two main models for PV cells and modules in the literature, i.e., single-diode [1]–[17] and double-diode [7], [18]–[26] models. These models differ in the accuracy and number of parameters involved in the calculation of PV current–voltage characteristics. It has been shown that the double-diode model is a more accurate model in representing the solar panel behavior as compared with the single-diode model, specifically at low irradiation levels [7], [18], [27]. To use these models in the simulation and evaluation of PV systems, one needs to determine the models parameters. However, parameter identification of such models is a challenging problem, since the derived equations for the estimation of a PV model parameters are implicit and nonlinear and may not be analytically solved. Moreover, the numerical solutions require appropriate initial values to achieve convergence.

Two main methods exist to extract the parameters of a PV double-diode model. The first method is based on fitting theoretical *I–V* curves to some of the experimental ones. In the other method, the parameters are determined using a few selected key points of the experimental data [4], [6], [7], [22], [23]. This approach is attractive in industrial applications because of its speed and need for few data from the *I–V* curves which are commonly available in the PV manufacturer catalogues. In this technique, to solve the resulting nonlinear equations, one needs a suitable initial point to make sure that the numerical iterations will converge. In [6], [7], and [20], some analytical solutions for the parameters of the double-diode model have been derived. However, these solutions need the slope of the *I–V* curves at the open-circuit point which is not normally given by the PV manufacturers.

This paper presents a new set of analytical solutions for the parameters of a five-parameter double-diode model of PV cells and modules which only require the coordinates of three key points of the *I–V* curves, i.e., the open-circuit $(0, V_{oc})$, the short circuit $(I_{sc}, 0)$ and the maximum power point (MPP) (I_m, V_m).These analytical solutions are successfully used in Newton–Raphson numerical iterations to achieve convergence and obtain more accurate solutions. It is shown that the extracted numerical and analytical solutions by the proposed method in this paper may serve as a suitable initial point for other approaches on the basis of curve-fitting techniques.

The remainder of this paper is organized as follows. In Section II, the original nonlinear equations of the double-diode model of PV panels are given. Section III deals with the derivation of initial point for the numerical solutions. In Section IV, the dependence of the PV module parameters on the operating condition is discussed. Section V illustrates the results by applying the proposed method to different PV modules, and proves the validity of the suggested parameter identification scheme in comparison with the experimental data. Finally, the concluding remarks are made in Section VI.

II. Derivation of Nonlinear Equations Used in Numerical Solutions

Fig. 1, shows the double-diode equivalent circuit of a PV *cell*. It should be noted that PV *modules* are manufactured from

Manuscript received July 13, 2013; revised February 10, 2014; accepted February 16, 2014. Date of publication March 5, 2014; date of current version April 18, 2014.

M. Hejri and M. R. Azizian are with the Department of Electrical Engineering, Sahand University of Technology, Tabriz 51335-1996, Iran (e-mail: hejri@sut.ac.ir; azizian@sut.ac.ir).

H. Mokhtari is with the Department of Electrical Engineering, Sharif University of Technology, Tehran 1392, Iran (e-mail: mokhtari@sharif.edu).

M. Ghandhari and L. Söder are with the Department of Electric Power Systems, School of Electrical Engineering, KTH-Royal Institute of Technology, Stockholm SE-100 44, Sweden (e-mail: mehrdad.ghandhari@ee.kth.se; lennart.soder@ee.kth.se).

Digital Object Identifier 10.1109/JPHOTOV.2014.2307161

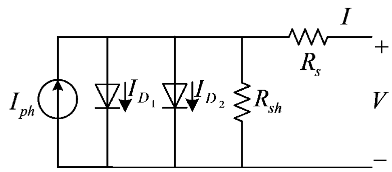

Fig. 1. Equivalent circuit of a double-diode model of a PV cell.

the series connection of PV cells to achieve high power and voltage levels. Moreover, some bypass diodes are installed in PV modules to avoid avalanche breakdown and hot spots during partial shading. It is a common practice to assume that the characteristics of the series cells inside a module are nearly identical [20], [28]. As a result, a PV module model is considered as a single cell with some multipliers that are incorporated in the cell model dependent upon the number of series-connected cells in the module. According to the equivalent circuit given in Fig. 1, the general PV panel current–voltage relationship in a specified illumination and temperature is given as

$$I = I_{ph} - I_{s1}\left[\exp\left(\frac{V+R_sI}{n_1N_sV_t}\right)-1\right] - I_{s2}\left[\exp\left(\frac{V+R_sI}{n_2N_sV_t}\right)-1\right] - \frac{V+R_sI}{R_{sh}} \quad (1)$$

where, I and V are the terminal current and voltage of the PV panel, I_{s1} is the saturation current due to diffusion mechanism, I_{s2} is the saturation current because of carrier recombination in space-charge region, n_1 diode ideality factor for diffusion current, n_2 diode ideality factor for generation-recombination current, N_s is the number of series-connected PV cells in the PV panel, R_s and R_{sh} are the series and shunt resistances, and V_t is cell thermal voltage defined as

$$V_t = \frac{kT}{q} \quad (2)$$

where k is Boltzmann's constant ($1.38 \times 10^{-23}\,\mathrm{J/K}$), q is the elementary charge ($1.6 \times 10^{-19}\,\mathrm{C}$), and T is p-n junction temperature in Kelvin. To reduce the complexity of the computations in practical cases, the values of the ideality factors are commonly approximated as $n_1 = 1$ and $n_2 = 2$ with a reasonable accuracy that is based on Shockley's diffusion theory [7], [19]–[23]. Although this assumption is widely used in the literature, however, it may not be always true [18], [29]. Therefore, (1) can be rewritten as

$$I = I_{ph} - I_{s1}\left[\exp\left(\frac{V+R_sI}{N_sV_t}\right)-1\right] - I_{s2}\left[\exp\left(\frac{V+R_sI}{2N_sV_t}\right)-1\right] - \frac{V+R_sI}{R_{sh}}. \quad (3)$$

Thus, the number of unknown parameters is reduced from 7 in (1) to 5 in (3). Our main goal is to determine the five parameters R_s, R_{sh}, I_{s1}, I_{s2}, and I_{ph} only based on the available data in a PV module datasheets.

Datasheet information is given for specified radiation and temperature conditions that is called as standard test condition (STC). In the STC, the radiation level is $1\,\mathrm{kW/m^2}$ with an air mass AM1.5 at the cell or module temperature of $25\,^\circ\mathrm{C}$ [8]. Available data in the manufactures datasheets are: the open-circuit voltage (V_{oc}), the short-circuit current (I_{sc}), the voltage at MPP (V_m), and the current at MPP (I_m).

Equation (1) is now evaluated at three points of the I–V curve of the PV module, i.e., the open circuit $(0, V_{oc})$, the short circuit $(I_{sc}, 0)$ and the MPP (I_m, V_m) as follows:

$$0 = I_{ph} - I_{s1}\left[\exp\left(\frac{V_{oc}}{N_sV_t}\right)-1\right] - I_{s2}\left[\exp\left(\frac{V_{oc}}{2N_sV_t}\right)-1\right] - \frac{V_{oc}}{R_{sh}} \quad (4)$$

$$I_{sc} = I_{ph} - I_{s1}\left[\exp\left(\frac{R_sI_{sc}}{N_sV_t}\right)-1\right] - I_{s2}\left[\exp\left(\frac{R_sI_{sc}}{2N_sV_t}\right)-1\right] - \frac{R_sI_{sc}}{R_{sh}} \quad (5)$$

$$I_m = I_{ph} - I_{s1}\left[\exp\left(\frac{V_m+R_sI_m}{N_sV_t}\right)-1\right] - I_{s2}\left[\exp\left(\frac{V_m+R_sI_m}{2N_sV_t}\right)-1\right] - \frac{V_m+R_sI_m}{R_{sh}}. \quad (6)$$

The power transferred at each point on the PV module I–V curve is given by

$$P = VI. \quad (7)$$

Next, the power term in (7) is differentiated with respect to V as follows:

$$\frac{dP}{dV} = \left(\frac{dI}{dV}\right)V + I. \quad (8)$$

The derivative of the power with respect to the voltage at the MPP is zero. Thus,

$$\frac{dI}{dV} = -\frac{I_m}{V_m}. \quad (9)$$

Next, the term $\frac{dI}{dV}$ is obtained by taking the derivative of (1) with respect to V as follows:

$$\frac{dI}{dV} = -\frac{I_{s1}}{N_sV_t}\left(1+R_s\frac{dI}{dV}\right)\exp\left(\frac{V+R_sI}{N_sV_t}\right) - \frac{I_{s2}}{2N_sV_t} \times \left(1+R_s\frac{dI}{dV}\right)\exp\left(\frac{V+R_sI}{2N_sV_t}\right) - \frac{1}{R_{sh}}\left(1+R_s\frac{dI}{dV}\right). \quad (10)$$

By substituting (10) into (9), the following equation is obtained:

$$\frac{I_m}{V_m} = \frac{I_{s1}}{N_sV_t}\left(1-R_s\frac{I_m}{V_m}\right)\exp\left(\frac{V_m+R_sI_m}{N_sV_t}\right) + \frac{I_{s2}}{2N_sV_t} \times \left(1-R_s\frac{I_m}{V_m}\right)\exp\left(\frac{V_m+R_sI_m}{2N_sV_t}\right) + \frac{1}{R_{sh}}\left(1-R_s\frac{I_m}{V_m}\right). \quad (11)$$

Using (4), one can write

$$I_{ph} = \frac{V_{\rm oc}}{R_{sh}} + I_{s1}\left[\exp\left(\frac{V_{\rm oc}}{N_s V_t}\right) - 1\right] + I_{s2}\left[\exp\left(\frac{V_{\rm oc}}{2N_s V_t}\right) - 1\right]. \quad (12)$$

Substituting (12) into (5) and (6) yields

$$I_{\rm sc} = I_{s1}\left[\exp\left(\frac{V_{\rm oc}}{N_s V_t}\right) - \exp\left(\frac{R_s I_{\rm sc}}{N_s V_t}\right)\right] + I_{s2}\left[\exp\left(\frac{V_{\rm oc}}{2N_s V_t}\right) - \exp\left(\frac{R_s I_{\rm sc}}{2N_s V_t}\right)\right] + \frac{V_{\rm oc} - R_s I_{\rm sc}}{R_{sh}} \quad (13)$$

$$I_m\left(1 + \frac{R_s}{R_{sh}}\right) = I_{s1}\left[\exp\left(\frac{V_{\rm oc}}{N_s V_t}\right) - \exp\left(\frac{V_m + R_s I_m}{N_s V_t}\right)\right] + I_{s2}\left[\exp\left(\frac{V_{\rm oc}}{2N_s V_t}\right) - \exp\left(\frac{V_m + R_s I_m}{2N_s V_t}\right)\right] + \frac{V_{\rm oc} - V_m}{R_{sh}}. \quad (14)$$

Equations (11), (13), and (14) are three independent equations with four unknown variables R_s, R_{sh}, I_{s1}, and I_{s2}. Therefore, one further equation is needed.

At the short-circuit point on the *I–V* curve, $I = I_{\rm sc}, V = 0, \frac{dI}{dV}|_{V=0} = -\frac{1}{R_{sho}}$. Substituting these values into (10) and after some mathematical manipulations, one can obtain

$$(R_{sho} - R_s)\left[\frac{1}{R_{sh}} + \frac{I_{s1}}{N_s V_t}\exp\left(\frac{R_s I_{\rm sc}}{N_s V_t}\right) + \frac{I_{s2}}{2N_s V_t}\exp\left(\frac{R_s I_{\rm sc}}{2N_s V_t}\right)\right] - 1 = 0. \quad (15)$$

Now, a new unknown variable R_{sho} is created.

As shown in [6], assuming $R_{sho}, R_{sh} \gg R_s$, and $\frac{I_{s1}}{N_s V_t}\exp(\frac{R_s I_{sc}}{N_s V_t}), \frac{I_{s2}}{2N_s V_t}\exp(\frac{R_s I_{sc}}{2N_s V_t}) \ll \frac{1}{R_{sh}}$, from (15) one can conclude that $R_{sho} \approx R_{sh}$. Therefore, (15) can be rewritten as

$$(R_{sh} - R_s)\left[\frac{1}{R_{sh}} + \frac{I_{s1}}{N_s V_t}\exp\left(\frac{R_s I_{\rm sc}}{N_s V_t}\right) + \frac{I_{s2}}{2N_s V_t}\exp\left(\frac{R_s I_{\rm sc}}{2N_s V_t}\right)\right] - 1 = 0. \quad (16)$$

Equations (11), (13), (14), and (16) are four independent equations with four unknown variables R_s, R_{sh}, I_{s1}, and I_{s2}. These equations can be solved by the Newton–Raphson method. However, as it will be shown in Section IV, because of the very small terms of I_{s1} and I_{s2} in the Jacobian matrix, this matrix is close to singularity and for some PV modules the Newton–Raphson method may not converge. To overcome this problem, I_{s1} and I_{s2} have been eliminated from (11), (13), (14), and (16) by applying some mathematical manipulations which result in a set of equations with only unknown variables of R_s, R_{sh}.

For PV modules, the approximations $\exp(\frac{V_{\rm oc}}{N_s V_t}) \gg \exp(\frac{R_s I_{\rm sc}}{N_s V_t})$ and $\exp(\frac{V_{\rm oc}}{2N_s V_t}) \gg \exp(\frac{R_s I_{\rm sc}}{2N_s V_t})$ are valid [7]. Therefore, (13) can be rewritten as

$$I_{\rm sc} = I_{s1}\exp\left(\frac{V_{\rm oc}}{N_s V_t}\right) + I_{s2}\exp\left(\frac{V_{\rm oc}}{2N_s V_t}\right) + \frac{V_{\rm oc} - R_s I_{\rm sc}}{R_{sh}}. \quad (17)$$

Solving the set of equations in (17) and (14) with respect to the unknown variables I_{s1} and I_{s2} yields

$$I_{s1} = \frac{a\exp(-\frac{V_{oc}}{2N_s v_t}) - b\exp(-\frac{V_m + R_s I_m}{2N_s v_t})}{\exp(\frac{V_{oc}}{2N_s v_t}) - \exp(\frac{V_m + R_s I_m}{2N_s v_t})} \quad (18)$$

$$I_{s2} = \frac{a\exp(-\frac{V_{oc}}{N_s v_t}) - b\exp(-\frac{V_m + R_s I_m}{N_s v_t})}{\exp(-\frac{V_{oc}}{2N_s v_t}) - \exp(-\frac{V_m + R_s I_m}{2N_s v_t})} \quad (19)$$

where, $a = (1 + \frac{R_s}{R_{sh}})I_{\rm sc} - \frac{V_{oc}}{R_{sh}}$ and $b = (1 + \frac{R_s}{R_{sh}})(I_{\rm sc} - I_m) - \frac{V_m}{R_{sh}}$.

By substituting (18) and (19) into (11) and (16) and after some mathematical manipulations one can obtain

$$\left[\frac{1}{R_{sh}}\left(1 - \frac{R_s I_m}{V_m}\right) - \frac{I_m}{V_m}\right]\left[2 - \exp\left(\frac{V_{\rm oc} - V_m - R_s I_m}{2N_s V_t}\right) - \exp\left(\frac{V_m - V_{\rm oc} + R_s I_m}{2N_s V_t}\right)\right] + \frac{1}{N_s V_t}\left(1 - \frac{R_s I_m}{V_m}\right) \times \left[-\left(\frac{a}{2} + b\right)\exp\left(\frac{-V_{\rm oc} + V_m + R_s I_m}{2N_s V_t}\right) + \frac{a}{2}\exp\left(\frac{-V_{\rm oc} + V_m + R_s I_m}{N_s V_t}\right) - \frac{b}{2}\exp\left(\frac{V_{\rm oc} - V_m - R_s I_m}{2N_s V_t}\right) + \frac{3b}{2}\right] = 0 \quad (20)$$

$$\frac{R_{sh} - R_s}{N_s V_t}\left[a\exp\left(\frac{R_s I_{\rm sc} - V_{\rm oc}}{N_s V_t}\right) - (a+b)\exp\left(\frac{R_s I_{\rm sc}}{N_s V_t} - \frac{V_m + V_{\rm oc} + R_s I_m}{2N_s V_t}\right) + b\exp\left(\frac{R_s I_{\rm sc}}{N_s V_t} - \frac{V_m + R_s I_m}{N_s V_t}\right) + \frac{a}{2}\exp\left(\frac{R_s I_{\rm sc} - V_{\rm oc}}{2N_s V_t}\right) - \frac{b}{2}\exp\left(\frac{V_{\rm oc} + R_s I_{\rm sc}}{2N_s V_t} - \frac{V_m + R_s I_m}{N_s V_t}\right) - \frac{a}{2}\exp\left(\frac{V_m + R_s I_m + R_s I_{\rm sc}}{2N_s V_t} - \frac{V_{\rm oc}}{N_s V_t}\right) + \frac{b}{2}\exp\left(\frac{R_s I_{\rm sc} - V_m - R_s I_m}{2N_s V_t}\right)\right] - \frac{R_s}{R_{sh}}\left[2 - \exp\left(\frac{V_{\rm oc} - V_m - R_s I_m}{2N_s V_t}\right) - \exp\left(\frac{V_m - V_{\rm oc} + R_s I_m}{2N_s V_t}\right)\right] = 0. \quad (21)$$

Now, (20) and (21) are a set of nonlinear equations with only two unknown variables R_s and R_{sh}. In Section IV, it is shown that the solution of (20), (21) is very close to the solution of (11), (13), (14), and (16). Therefore, (20), (21) can be used instead of (11), (13), (14), and (16). To solve these equations numerically, one needs a good initial point. We obtain a set of approximate analytical solutions and use them as a candidate for the initial point. In the next section, it is shown how these initial points can be derived based on reasonable assumptions.

III. Derivation of Analytical Solutions as an Initial Point

Considering $R_{sh} \gg R_s$ [7], $1 + \frac{R_s}{R_{sh}}$ is approximated by 1. In addition, according to the typical available values for the PV module parameters in the datasheets and literatures [6], the approximations $I_{\rm sc} \gg \frac{V_{\rm oc}}{R_{sh}}, I_{\rm sc} - I_m \gg \frac{V_m}{R_{sh}}$ are valid. According to these reasonable assumptions, the terms $a = (1 + \frac{R_s}{R_{sh}})I_{\rm sc} - \frac{V_{\rm oc}}{R_{sh}}$ and $b = (1 + \frac{R_s}{R_{sh}})(I_{\rm sc} - I_m) - \frac{V_m}{R_{sh}}$ are approximated with $a = I_{\rm sc}$ and $b = I_{\rm sc} - I_m$. Thus, they become independent of R_s and R_{sh}. The term $\frac{1}{R_{sh}}(1 - \frac{R_s I_m}{V_m}) - \frac{I_m}{V_m}$ in (20) is also estimated as $-\frac{I_m}{V_m}$. According to these simplifications, (18) and (19) can be rewritten as

$$I_{s1} = \frac{I_{\rm sc}\exp(-\frac{V_{\rm oc}}{2N_s v_t}) - (I_{\rm sc} - I_m)\exp(-\frac{V_m + R_s I_m}{2N_s v_t})}{\exp(\frac{V_{\rm oc}}{2N_s v_t}) - \exp(\frac{V_m + R_s I_m}{2N_s v_t})} \quad (22)$$

$$I_{s2} = \frac{I_{\rm sc}\exp(-\frac{V_{\rm oc}}{N_s v_t}) - (I_{\rm sc} - I_m)\exp(-\frac{V_m + R_s I_m}{N_s v_t})}{\exp(-\frac{V_{\rm oc}}{2N_s v_t}) - \exp(-\frac{V_m + R_s I_m}{2N_s v_t})}. \quad (23)$$

Also, (20) is simplified as

$$\begin{aligned} -\frac{I_m}{V_m}&\left[2 - \exp\left(\frac{V_{\rm oc} - V_m - R_s I_m}{2N_s V_t}\right)\right. \\ &\left. - \exp\left(\frac{V_m - V_{\rm oc} + R_s I_m}{2N_s V_t}\right)\right] + \frac{1}{N_s V_t}\left(1 - \frac{R_s I_m}{V_m}\right) \\ &\times\left[-\left(\frac{3I_{\rm sc}}{2} - I_m\right)\exp\left(\frac{-V_{\rm oc} + V_m + R_s I_m}{2N_s V_t}\right)\right. \\ &+ \frac{I_{\rm sc}}{2}\exp\left(\frac{-V_{\rm oc} + V_m + R_s I_m}{N_s V_t}\right) - \frac{I_{\rm sc} - I_m}{2} \\ &\left.\times\exp\left(\frac{V_{\rm oc} - V_m - R_s I_m}{2N_s V_t}\right) + \frac{3(I_{\rm sc} - I_m)}{2}\right] = 0. \quad (24) \end{aligned}$$

We use the first-, second-, and third-order approximations $\exp(kR_s) = 1 + kR_s, \exp(kR_s) = 1 + kR_s + k^2R_s^2/2$, and $\exp(kR_s) = 1 + kR_s + k^2R_s^2/2 + k^3R_s^3/6$ to transform the exponential terms in (24) to polynomial ones. Therefore, the following quadratic, cubic, and quartic equations are obtained:

$$\begin{aligned} A_2R_s^2 + B_2R_s + C_2 &= 0 \\ A_3R_s^3 + B_3R_s^2 + C_3R_s + D_3 &= 0 \\ A_4R_s^4 + B_4R_s^3 + C_4R_s^2 + D_4R_s + E_4 &= 0. \end{aligned} \quad (25)$$

Coefficients $A_i, B_i, C_i, i \in \{2, 3, 4\}, D_3, D_4, E_4$ are provided in Appendix. Comparing the calculated coefficients to each other, one can obtain

$$\begin{aligned} E_4 &= D_3 = C_2 \\ D_4 &= C_3 = B_2 \\ C_4 &= B_3. \end{aligned} \quad (26)$$

After analytical solving of the proposed classic equations in (25) and obtaining a feasible solution for R_s, one can substitute it into (22) and (23) to compute the saturation currents I_{s1} and I_{s2}. Next, an estimation of R_{sh} is calculated by (16). This equation can be rewritten in the following form:

$$\begin{aligned} R_{sh}(R_{sh} - R_s)&\left[\frac{1}{R_{sh}} + \frac{I_{s1}}{N_s V_t}\exp\left(\frac{R_s I_{\rm sc}}{N_s V_t}\right)\right. \\ &\left. + \frac{I_{s2}}{2N_s V_t}\exp\left(\frac{R_s I_{\rm sc}}{2N_s V_t}\right)\right] - R_s = 0. \quad (27) \end{aligned}$$

Since $R_{sh} \gg R_s$, from (27), one can obtain

$$R_{sh} = \sqrt{\frac{R_s}{\frac{I_{s1}}{N_s V_t}\exp(\frac{R_s I_{\rm sc}}{N_s V_t}) + \frac{I_{s2}}{2N_s V_t}\exp(\frac{R_s I_{\rm sc}}{2N_s V_t})}} \quad (28)$$

where I_{s1} and I_{s2} are calculated via (22) and (23). Therefore, (25), (22), (23), and (28) provide approximate analytical solutions, and at the same time they are suitable initial points for the implicit nonlinear equations of (11), (13), (14), and (16) or (20), (21).

A comprehensive discussion on the analytic solution of the cubic and quartic equations in (25) can be found in any classic book on the theory of equations [30]. Based on the Abel–Ruffini theorem, the quartic or the fourth-order equation is the highest degree of a general polynomial for which the analytical solutions based on radicals can be found [31].

Note that in (11), (13), (14), and (16) or (20), (21), the parameter I_{ph} is eliminated, and therefore, it needs no initial value. However, one can find a good estimation of this parameter via (5). This equation can be rewritten as

$$\begin{aligned} I_{ph} = I_{\rm sc} + I_{s1}&\left[\exp\left(\frac{R_s I_{\rm sc}}{N_s V_t}\right) - 1\right] \\ &+ I_{s2}\left[\exp\left(\frac{R_s I_{\rm sc}}{2N_s V_t}\right) - 1\right] + \frac{R_s I_{\rm sc}}{R_{sh}}. \quad (29) \end{aligned}$$

Now, since $I_{\rm sc}$ is much greater than the other terms on the right-hand side of (29), therefore, the value of I_{ph} is estimated as $I_{\rm sc}$.

A. Zero Series Resistance Initial Condition

As it will be shown in Section IV, sometimes during parameter determination of the PV modules, the algebraic equations in (25) do not result in any feasible solution for the series resistance. It means that the proposed real positive solutions for R_s in (25) do not yield any feasible initial point that makes the numerical solutions of (11), (13), (14), and (16) or (20), (21) converge. This problem is appeared for the PV modules with a small series resistance. In such cases, the initial value of R_s is set to zero. Since setting $R_s = 0$ results in nonfeasible solution of $R_{sh} = 0$ in (28), the value of R_{sh} is estimated via (21). Assuming $R_s = 0$, the parameters $a = (1 + \frac{R_s}{R_{sh}})I_{\rm sc} - \frac{V_{\rm oc}}{R_{sh}}$ and $b = (1 + \frac{R_s}{R_{sh}})(I_{\rm sc} - I_m) - \frac{V_m}{R_{sh}}$ in (21) are simplified as $a = I_{\rm sc} - \frac{V_{\rm oc}}{R_{sh}}$ and $b = I_{\rm sc} - I_m - \frac{V_m}{R_{sh}}$. Now, setting $R_s = 0$ and substituting parameters a, b into (21) and after some mathematical manipulations one can obtain

$$R_{sh} = \frac{N}{D} \quad (30)$$

where

$$D = I_{\rm sc}\exp\left(-\frac{V_{\rm oc}}{N_sV_t}\right) - (2I_{\rm sc}-I_m)\exp\left(-\frac{V_{\rm oc}+V_m}{2N_sV_t}\right)$$
$$+ (I_{\rm sc}-I_m)\exp\left(\frac{V_m}{N_sV_t}\right) + \frac{I_{\rm sc}}{2}\exp\left(-\frac{V_{\rm oc}}{2N_sV_t}\right)$$
$$- \frac{I_{\rm sc}-I_m}{2}\exp\left(\frac{V_{\rm oc}}{2N_sV_t}-\frac{V_m}{N_sV_t}\right) - \frac{I_{\rm sc}}{2}$$
$$\times \exp\left(\frac{V_m}{2N_sV_t}-\frac{V_{\rm oc}}{N_sV_t}\right) + \frac{I_{\rm sc}-I_m}{2}\exp\left(-\frac{V_m}{2N_sV_t}\right)$$
$$N = V_{\rm oc}\exp\left(-\frac{V_{\rm oc}}{N_sV_t}\right) - (V_m+V_{\rm oc})\exp\left(-\frac{V_{\rm oc}+V_m}{2N_sV_t}\right)$$
$$+ V_m\exp\left(-\frac{V_m}{N_sV_t}\right) + \frac{V_{\rm oc}}{2}\exp\left(-\frac{V_{\rm oc}}{2N_sV_t}\right)$$
$$- \frac{V_m}{2}\exp\left(\frac{V_{\rm oc}}{2N_sV_t}-\frac{V_m}{N_sV_t}\right)$$
$$- \frac{V_{\rm oc}}{2}\exp\left(-\frac{V_m}{2N_sV_t}-\frac{V_{\rm oc}}{N_sV_t}\right)+\frac{V_m}{2}\exp\left(-\frac{V_m}{2N_sV_t}\right).$$

Therefore in cases that (25) do not suggest any feasible value for R_s, the initial values of $R_s = 0$ and R_{sh} in (29) are used for the numerical solution of (20), (21). Now, an idea arises that one can use the proposed estimated values of R_s and R_{sh}, to obtain an approximate value of saturation currents I_{s1}, I_{s2} via (18) and (19). However, as it will be shown in Section IV, the proposed initial values for R_s and R_{sh} do not guarantee reasonable values for I_{s1} or I_{s2}. It means that they may result unrealistic negative values in (18), (19). However, it does not matter, because the numerical solution of (20), (21) is independent from the parameters I_{s1} and I_{s2}.

IV. Dependence of the Parameters on the Temperature and Irradiation Levels

The information in PV manufacturers' catalogues refers to the STC, and therefore, the parameter identified from the datasheets is valid only under the STC. However, generally the dependence of the PV model parameters on T and G can be inserted in the mathematical model via a set of suitable translational formulas. With this approach, the current–voltage (*I–V*) relationship which considers the irradiance and temperature conditions is realized. Mathematically, in this relationship, the dependence on the temperature and irradiation levels is taken into account by using the principle of supervision [2], [28]. In this paper, for R_s, R_{sh}, and I_{s1}, the same relations in [2], [32] are used as

$$R_s = R_{\rm STC} \tag{31}$$

$$R_{sh} = R_{sh,\rm STC}\frac{G_{\rm STC}}{G} \tag{32}$$

$$\frac{I_{s1}}{I_{s1,\rm STC}} = \left[\frac{T}{T_{\rm STC}}\right]^3 \exp\left[\frac{1}{k}\left(\frac{E_{g,\rm STC}}{T_{\rm STC}}-\frac{E_g}{T}\right)\right] \tag{33}$$

where the subscript $_{\rm STC}$ stands for the values of different parameters in STC. E_g is the material band gap energy and its value in $T_{\rm STC} = 25$ °C is set to 1.121 eV for silicon cells [2], [32].

TABLE I
Datasheet Values and Identified Parameters of the PV Module KC200GT Via the Numerical Solution of (11), (13), (14), and (16)

Datasheet values in STC	Module KC200GT [34]		
V_{oc}(V)	32.9		
I_{sc}(A)	8.21		
$V_m(V)$	26.3		
$I_m(A)$	7.61		
$P_m(W)$	200		
N_s	54		
Roots of quadratic equation in (25)			
Solutions	-1.5959&0.2280		
Roots of cubic equation in (25)			
Solutions	-1.1216&0.5347&0.3597		
Roots of quartic equation in (25)			
Solutions	-1.2021&0.4082 $\pm$ 0.7987i&0.2797		
Analytical and numerical solutions based on the feasible solution of the quadratic equation in (25)			
Parameters	Numerical	Analytical	Error(%)
$R_s(\Omega)$	0.3181	0.2280	28.3049
$R_{sh}(\Omega)$	278.9106	135.5209	51.4106
$I_{s1}(nA)$	0.3795	0.2915	23.1838
$I_{s2}(\mu A)$	4.4334	17.5582	-296.0359
$I_{ph}(A)$	8.2193	8.2100	0.1140

The value of E_g as a function of the cell temperature is given by [2], [32]

$$\frac{E_g}{E_{g,T_{\rm STC}}} = 1 - 0.0002677(T - T_{\rm STC}). \tag{34}$$

The dependence of the photo current on the temperature and irradiation level can be stated as [28]

$$\frac{I_{ph}}{I_{ph,\rm STC}} = \frac{G}{G_{\rm STC}}[1 + k_i(T - T_{\rm STC})] \tag{35}$$

where $k_i(\%/°\mathrm{C})$ is the temperature coefficient of the short-circuit current.

In [33], a proportional relation for I_{s2} as a function of the cell temperature has been developed as

$$I_{s2} \propto T^{\frac{5}{2}}\exp\left(-\frac{E_g}{2kT}\right). \tag{36}$$

By proposing the proportional constant C, (36) can be written as

$$I_{s2} = CT^{\frac{5}{2}}\exp\left(-\frac{E_g}{2kT}\right). \tag{37}$$

Evaluating (37) at STC and after some algebra, one can obtain

$$\frac{I_{s2}}{I_{s2,\rm STC}} = \left[\frac{T}{T_{\rm STC}}\right]^{\frac{5}{2}}\exp\left[\frac{1}{2k}\left(\frac{E_{g,\rm STC}}{T_{\rm STC}}-\frac{E_g}{T}\right)\right]. \tag{38}$$

Therefore, the parameters in (31), (32), (33), (35), and (38) can be inserted into (3) to extract the PV module *I–V* curves in different operating conditions.

V. Evaluation of the Results

Two case studies are studied in this section. The first case is the PV module KC200GT [34] with a high value of the series resistance, and the second one is the PV module GEPV110 [35] with a small value of the series resistance. The datasheet parameters of the PV module KC200GT in STC is given in

TABLE II
IDENTIFIED PARAMETERS FOR THE PV MODULE KC200GT VIA THE NUMERICAL SOLUTION OF (20), (21) AND THE METHOD IN [20]

Parameters	(20-21)	The approach in [20]
$R_s(\Omega)$	0.3181	0.1797
$R_{sh}(\Omega)$	278.9255	177.0234
$I_{s1}(nA)$	0.3795	0.3032
$I_{s2}(\mu A)$	4.4330	13.9731
$I_{ph}(A)$	8.2193	8.1959

Table I. This table also shows the solutions of the quadratic, cubic, and quartic equations in (25). The term Error(%) in this table is the relative error between the accurate numerical and approximate analytical solutions as the initial point which is given by

$$\text{Error}(\%) = \frac{X_{\text{numerical}} - X_{\text{analytical}}}{X_{\text{numerical}}} \times 100 \qquad (39)$$

where $X_{\text{numerical}}$ is the estimated parameter by the numerical solutions and $X_{\text{analytical}}$ is the estimated parameter by the approximate analytical solution.

The identified parameters for five-parameter model in this table are extracted from the numerical solutions of (11), (13), (14), and (16) including I_{s1} and I_{s2}. The proposed analytical solutions serve as a suitable initial point for the convergence of the numerical iterations. Table II provides the identified parameters for the PV module of Table I via the numerical solution of (20), (21) excluding the saturation currents I_{s1} and I_{s2}. The required initial values for numerical solving of (20), (21) are the same as those required for the analytical solution of R_s and R_{sh} in Table I. Comparing the results of Tables I and II, one can see that there is a good agreement between the numerical solution of the set of equations in (20), (21) and (11), (13), (14), (16). This confirms the reasonable approximations $\exp(\frac{V_{oc}}{N_s V_t}) \gg \exp(\frac{R_s I_{sc}}{N_s V_t})$ and $\exp(\frac{V_{oc}}{2N_s V_t}) \gg \exp(\frac{R_s I_{sc}}{2N_s V_t})$ which are used to derive (20, (21) from (11), (13, (14), and (16). This means that one can use (20, (21) rather than (11), (13), (14), and (16) in the numerical analysis with an acceptable degree of accuracy and convergence reliability. The proposed approach in this study is compared with the curve-fitting technique proposed in [20]. The identification procedure in [20] utilizes the Levenberg–Marquardt optimization method to obtain a solution for the parameters of the five-parameter double-diode model in (3). To start the Levenberg–Marquardt method, one needs to determine the appropriate initial point. However, the proposed initial values in [20] need the slope of the *I–V* curves at the short-circuit and the open-circuit points which are not available in the manufacturer catalogues. As a consequence, for the implementation of the method, the proposed analytical and numerical solutions in this study are used as the initial point for the proposed method in [20]. In the case of PV module KC200GT, the proposed analytical and numerical solutions in Table I are accurate enough to achieve a convergence in the Levenberg–Marquardt method. Fig. 2 presents the simulated *I–V* curves for the proposed approach in this study and the method proposed in [20] in conjunction with the experimental data in different irradiation levels for the PV module KC200GT. Table II provides the estimated parameters by the curve-fitting technique in [20]

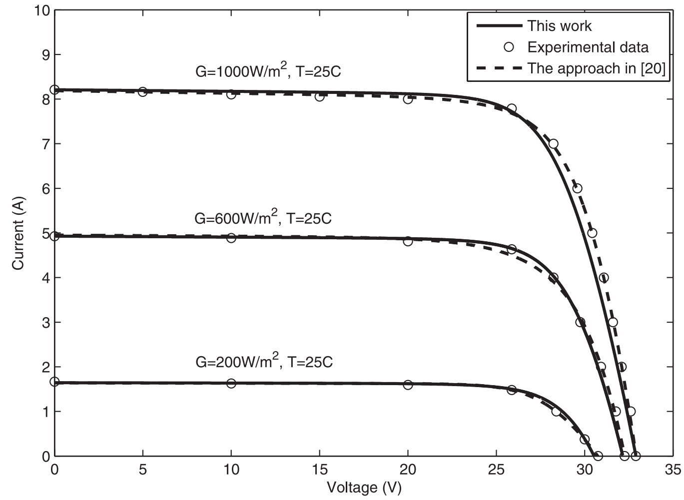

Fig. 2. Experimental data and theoretical *I–V* curves for the PV module KC200GT.

TABLE III
EVALUATION OF nRMSE(%) FOR THE PV MODULE KC200GT VIA THE NUMERICAL SOLUTION OF (20), (21) AND THE METHOD IN [20]

Irradiation level $G(W/m^2)$ and cell temperature $T(°C)$			
	$G = 1000$ $T = 25$	$G = 600$ $T = 25$	$G = 200$ $T = 25$
$nRMSE(\%)$ This work	6.35	4.36	6.55
$nRMSE(\%)$ The method in [20]	1.12	2.15	1.29

in STC. Table III gives the corresponding normalized root mean square error percentage [nRMSE(%)] calculated by

$$\text{nRMSE}(\%) = \frac{\sqrt{\frac{1}{N}\sum_{i=1}^{N}(E_i - M_i)^2}}{\sqrt{\frac{1}{N}\sum_{i=1}^{N} M_i^2}} \times 100 \qquad (40)$$

where N is the number of measurements, E_i is the estimated value, and M_i represents the measured data. As it can be seen from this table, the curve-fitting approach exhibits lower nRMSE(%). This observation is expected because the curve-fitting methods use the whole data of the *I–V* curves, in our study only three remarkable points of the *I–V* curve are used for the parameter identification. These results show that the proposed approach has comparable accuracy levels but requires less data. During testing of the proposed parameter identification technique on different PV module datasheets, it has been observed that for some PV modules, the algebraic equations in (25) do not result in any suitable value for R_s, i.e., no feasible initial point was found to solve the set of equations in (11), (13), (14), (16) or in (20), (21). In Table IV, the parameters of the PV module GEPV110 are given in the STC. This table also contains the solutions of the algebraic equations in (25). None of the given real positive numbers for R_s resulted in any feasible initial point. Therefore, as it was mentioned in Section III-A, R_s is set to zero, and the value of R_{sh} in (29) is chosen as an initial point for the numerical analysis of (20), (21). As it can be seen from this table, substituting the proposed initial values of

TABLE IV
DATASHEET VALUES OF THE PV MODULE GEPV110 AND IDENTIFIED PARAMETERS VIA NUMERICAL SOLUTION OF (20), (21)

Datasheet values in STC	Module GEPV110 [35]		
V_{oc}(V)	21.2		
I_{sc}(A)	7.40		
$V_m(V)$	16.7		
$I_m(A)$	6.60		
$P_m(W)$	110		
N_s	36		
Roots of quadratic equation in (25)			
Solutions	$0.1490 \pm 0.1449i$		
Roots of cubic equation in (25)			
Solutions	$0.6494\&0.0871 \pm 0.1579i$		
Roots of quartic equation in (25)			
Solutions	$0.4450 \pm 0.6055i$ & $0.0922 \pm 0.1617i$		
Analytical and numerical solutions based on the feasible solution of the quadratic equation in (25)			
Parameters	Numerical	Analytical	Error(%)
$R_s(\Omega)$	0.2141	0.0000	100.0000
$R_{sh}(\Omega)$	83.7702	22.2605	73.4266
$I_{s1}(nA)$	0.5486	0.7227	-31.7292
$I_{s2}(\mu A)$	24.0448	-0.0014	100.0000
$I_{ph}(A)$	7.4188	7.4000	0.2547

TABLE V
IDENTIFIED PARAMETERS FOR THE PV MODULE GEPV110 VIA THE NUMERICAL SOLUTION OF (20), (21) AS THE INITIAL VALUE FOR (11), (13), (14), AND (16)

Parameters	GEPV110
$R_s(\Omega)$	0.2141
$R_{sh}(\Omega)$	83.7598
$I_{s1}(nA)$	0.5486
$I_{s2}(\mu A)$	24.0505
$I_{ph}(A)$	7.4189

R_s and R_{sh} into (18), (19) results in unrealistic negative value for I_{s2}. However, this does not affect our method since only the initial values for R_s and R_{sh} are required to solve (20), (21).

From Table IV, one can see, even though there is a large difference between the accurate numerical and the proposed initial values of $R_s = 0$ and R_{sh} in (29), the convergence is however successfully achieved. This reflects some kind of robustness with respect to the initial point in (20), (21) as compared with (11), (13), (14), and (16).

As it was shown in Tables I and II, the numerical solutions of the nonlinear equations in (20), (21) are very close to the ones of (11), (13), (14), and (16). Therefore, in cases that the numerical iterations in (11), (13), (14), and (16) fail to converge, one can use the equations in (20), (21) to obtain a solution with enough accuracy. The main reason for the high possibility of the numerical divergence in the set of equations in (11), (13), (14), and (16) is due to the high sensitivity of these equations to the accuracy of the initial guess. This stems from the existing of the very small terms I_{s1} and I_{s2} in the Jacobian matrix and the high dimension of the parameter space in the set of equations in (11), (13), (14), and (16) as compared with the set of equations in (20), (21) [4]. Another idea is to use the proposed numerical solution of (20, (21) as an initial point for (11), (13), (14), and (16). The results are shown in Table V.

As it can be seen from this table, the solutions are very close to the values presented in Table IV, and again, this confirms the consistency of the numerical solutions between the set of equations in (20), (21) and (11), (13), (14), and (16). In the case of the PV module GEPV110, the application of the curve-fitting approach in [20] does not result in further improvements in the numerical solutions that are suggested in Tables IV and V. There are two main reasons for this fact. The first reason is the proposed solutions in this study are so accurate that they are equal with the global optimal solutions of the curve-fitting optimization–based approach in case PV module GEPV110. The second reason is since the resulting optimization problem for the parameter extraction of PV cells and modules is highly nonlinear and a nonconvex problem, the conventional Newton–Raphson-based approaches like Levenberg–Marquardt tend to get stuck with the local optimal solutions that have been suggested by the proposed approach in this paper as the initial values. Fig. 3 shows the theoretical *I–V* curves for the PV module GEPV110 which is plotted along with the experimental data taken from the published *I–V* curve in the manufacturer datasheets. Table VI gives the evaluated nRMSE(%) corresponding to the theoretical *I–V* curves and experimental data. It can be observed that the theoretical *I–V* curves are sufficiently accurate for the experimental data. This proves the validity of the proposed parameter identification technique for PV modules.

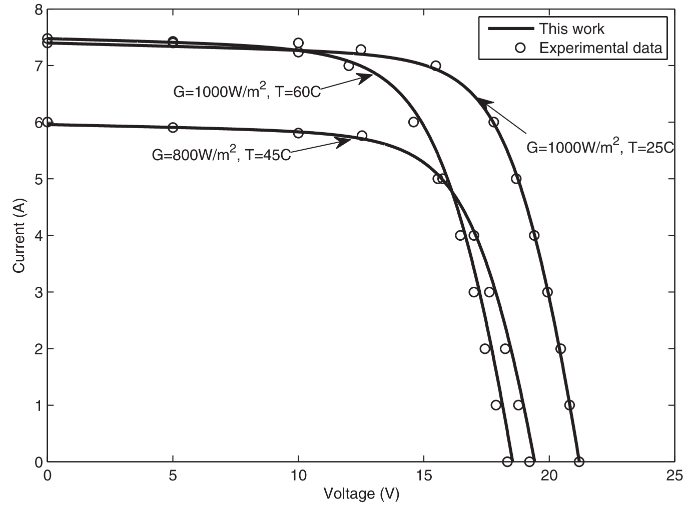

Fig. 3. Experimental data and theoretical *I–V* curves for the PV module GEPV110.

TABLE VI
EVALUATION OF NRMSE(%) FOR THE PV MODULE GEPV110 VIA THE NUMERICAL SOLUTION OF (20), (21)

Irradiation level $G(W/m^2)$ and cell temperature $T(°C)$			
	$G = 1000$ $T = 25$	$G = 800$ $T = 45$	$G = 1000$ $T = 60$
$nRMSE(\%)$ This work	1.29	6.05	6.73

VI. CONCLUSION

A new set of approximate analytical solutions for the extraction of double-diode model parameters that are based on only manufacturer datasheet values has been derived. The PV current–voltage relationship is evaluated at three key points namely, the open circuit, the short circuit, and the MPP to obtain

(4), (6). Moreover, the derivative of the PV power with respect to the voltage is made equal to zero at the MPP as the fourth equation in (11). The fifth equation in (16) is derived on the basis of the evaluation of the slope of the *I–V* curve at the short-circuit point via the assumption $R_{sh} \approx R_{sho}$. Next, the resulting nonlinear set of five equations in (4), (6), (11), and (16) with five unknown variables $R_s, R_{sh}, I_{s1}, I_{s2}$, and I_{ph} is simplified on the basis of the reasonable assumptions which are valid in PV cells and modules with a high degree of accuracy. The simplified set of equations in (22), (23), (25), and (28), (29) is solved to obtain a set of approximate analytical solutions. It has been shown that these solutions are suitable candidates as initial points for the numerical analysis of the original equations that are based on the Newton–Raphson method. The validity of the theoretical *I–V* curves has been evaluated by comparing the results with those obtained based on the experimental data. It is shown that the simulated *I–V* curves are sufficiently accurate.

Appendix
Coefficients in (25) and (26)

In the following formulations, $a = I_{\rm sc}$ and $b = I_{\rm sc} - I_m$.

$$\begin{aligned}
A_2 &= \frac{I_m^2}{2N_s^2V_t^2V_m}\left[\left(b+\frac{a}{2}\right)\exp\left(\frac{V_m-V_{\rm oc}}{2N_sV_t}\right)\right.\\
&\quad\left. - a\exp\left(\frac{V_m-V_{\rm oc}}{N_sV_t}\right) - \frac{b}{2}\exp\left(\frac{V_{\rm oc}-V_m}{2N_sV_t}\right)\right]\\
B_2 &= \frac{I_m^2}{2N_sV_tV_m}\left[\exp\left(\frac{V_m-V_{\rm oc}}{2N_sV_t}\right) - \exp\left(\frac{V_{\rm oc}-V_m}{2N_sV_t}\right)\right]\\
&\quad - \frac{I_m}{N_sV_t}\left(b+\frac{a}{2}\right)\left(\frac{1}{2N_sV_t}-\frac{1}{V_m}\right)\exp\left(\frac{V_m-V_{\rm oc}}{2N_sV_t}\right)\\
&\quad + \frac{aI_m}{2N_sV_t}\left(\frac{1}{N_sV_t}-\frac{1}{V_m}\right)\exp\left(\frac{V_m-V_{\rm oc}}{N_sV_t}\right)\\
&\quad + \frac{bI_m}{2N_sV_t}\left(\frac{1}{2N_sV_t}+\frac{1}{V_m}\right)\exp\left(\frac{V_{\rm oc}V_m}{2N_sV_t}\right) - \frac{3bI_m}{2N_sV_tV_m}\\
C_2 &= -\frac{2I_m}{V_m} + \frac{3b}{2N_sV_t} + \left(\frac{I_m}{V_m} - \frac{1}{N_sV_t}\left(b+\frac{a}{2}\right)\right)\\
&\quad \times\exp\left(\frac{V_m-V_{\rm oc}}{2N_sV_t}\right) + \left(\frac{I_m}{V_m} - \frac{b}{2N_sV_t}\left(b+\frac{a}{2}\right)\right)\\
&\quad \times\exp\left(\frac{V_{\rm oc}-V_m}{2N_sV_t}\right) + \frac{a}{2N_sV_t}\exp\left(\frac{V_m-V_{\rm oc}}{N_sV_t}\right)\\
A_3 &= \frac{I_m^3}{8N_s^3V_t^3V_m}\left(b+\frac{a}{2}\right)\exp\left(\frac{V_m-V_{\rm oc}}{2N_sV_t}\right)\\
&\quad - \frac{aI_m^3}{4V_mN_s^3V_t^3}\exp\left(\frac{V_m-V_{\rm oc}}{N_sV_t}\right) + \frac{bI_m^3}{16V_mN_s^3V_t^3}\exp\left(\frac{V_{\rm oc}-V_m}{2N_sV_t}\right)\\
B_3 &= \frac{I_m^3}{2V_m\left(2N_sV_t\right)^2}\left[\exp\left(\frac{V_{\rm oc}-V_m}{2N_sV_t}\right) + \exp\left(\frac{V_m-V_{\rm oc}}{2N_sV_t}\right)\right]\\
&\quad - \frac{I_m^2}{2N_s^2V_t^2}\left(b+\frac{a}{2}\right)\exp\left(\frac{V_m-V_{\rm oc}}{2N_sV_t}\right)\left(\frac{1}{4N_sV_t}-\frac{1}{V_m}\right)\\
&\quad + \frac{aI_m^2}{2N_s^2V_t^2}\left(\frac{1}{2N_sV_t}-\frac{1}{V_m}\right)\exp\left(\frac{V_m-V_{\rm oc}}{N_sV_t}\right)\\
&\quad - \frac{bI_m^2}{\left(2N_sV_t\right)^2}\left(\frac{1}{4N_sV_t}+\frac{1}{V_m}\right)\exp\left(\frac{V_{\rm oc}-V_m}{2N_sV_t}\right)\\
D_3 &= -\frac{2I_m}{V_m} + \frac{3b}{2N_sV_t} + \left(\frac{I_m}{V_m} - \frac{1}{N_sV_t}\left(b+\frac{a}{2}\right)\right)\\
&\quad \times\exp\left(\frac{V_m-V_{\rm oc}}{2N_sV_t}\right) + \left(\frac{I_m}{V_m} - \frac{b}{2N_sV_t}\left(b+\frac{a}{2}\right)\right)\\
&\quad \times\exp\left(\frac{V_{\rm oc}-V_m}{2N_sV_t}\right) + \frac{a}{2N_sV_t}\exp\left(\frac{V_m-V_{\rm oc}}{N_sV_t}\right)\\
A_4 &= \frac{I_m^4}{6V_m\left(2N_sV_t\right)^4}\left[(a+2b)\exp\left(\frac{V_m-V_{\rm oc}}{2N_sV_t}\right)\right.\\
&\quad\left. - b\exp\left(\frac{V_{\rm oc}-V_m}{2N_sV_t}\right)\right] - \frac{aI_m^4}{12N_s^4V_t^4V_m}\exp\left(\frac{V_m-V_{\rm oc}}{N_sV_t}\right)\\
B_4 &= \frac{I_m^4}{6V_m\left(2N_sV_t\right)^3}\left[\exp\left(\frac{V_m-V_{\rm oc}}{2N_sV_t}\right) - \exp\left(\frac{V_{\rm oc}-V_m}{2N_sV_t}\right)\right]\\
&\quad - \frac{I_m^3}{\left(2N_sV_t\right)^3}\left(\frac{1}{6N_sV_t}-\frac{1}{V_m}\right)\left(b+\frac{a}{2}\right)\exp\left(\frac{V_m-V_{\rm oc}}{2N_sV_t}\right)\\
&\quad + \frac{b}{2}\frac{I_m^3}{\left(2N_sV_t\right)^3}\left(\frac{1}{6N_sV_t}+\frac{1}{V_m}\right)\exp\left(\frac{V_{\rm oc}-V_m}{2N_sV_t}\right)\\
&\quad + \frac{aI_m^3}{4N_s^3V_t^3}\left(\frac{1}{3N_sV_t}-\frac{1}{V_m}\right)\exp\left(\frac{V_m-V_{\rm oc}}{N_sV_t}\right).
\end{aligned}$$

References

[1] G. Tina, "A coupled electrical and thermal model for photovoltaic modules," *J. Sol. Energy Eng.*, vol. 132, no. 2, pp. 1–5, May 2010.

[2] M. T. Boyd, S. A. Klein, D. T. Reindl, and B. P. Dougherty, "Evaluation and validation of equivalent circuit photovoltaic solar cell performance models," *J. Sol. Energy Eng.*, vol. 133, no. 2, pp. 1–13, May 2011.

[3] J. Accarino, G. Petrone, C. Ramos-Paja, and G. Spagnuolo, "Symbolic algebra for the calculation of the series and parallel resistances in PV module model," in *Proc. Int. Conf. Clean Electr. Power*, Jun. 11–13, 2013, pp. 62–66.

[4] M. Hejri, H. Mokhtari, M. R. Azizian, and L. Söder. (2013). An analytical-numerical approach for parameter determination of a five-parameter single-diode model of photovoltaic cells and modules. *Int. J. Sustainable Energy* [Online]. Available: http://dx.doi.org/10.1080/14786451.2013.863886

[5] M. A. de Blas, J. L. Torres, E. Prieto, and A. Garcia, "Selecting a suitable model for characterizing photovoltaic devices," *Renewable Energy*, vol. 25, pp. 371–380, 2002.

[6] J. C. H. Phang, D. S. H. Chan, and J. R. Phillips, "Accurate analytical methods for the extraction of solar cell model parameters," *Electron. Lett.*, vol. 20, no. 10, pp. 406–408, May 1984.

[7] D. S. H. Chan and J. C. H. Phang, "Analytical methods for the extraction of solar-cell single and double diode model parameters from I–V characteristics," *IEEE Trans. Electron Devices*, vol. 34, no. 2, pp. 286–293, Feb. 1987.

[8] M. G. Villalva, J. R. Gazoli, and E. R. Filho, "Comprehensive approach to modeling and simulation of photovoltaic arrays," *IEEE Trans. Power Electron.*, vol. 24, no. 5, pp. 1198–1208, May 2009.

[9] K. Bouzidi, M. Chegaar, and A. Bouhemadou, "Solar cells parameters evaluation considering the series and shunt resistance," *Sol. Energy Mater. Sol. Cells*, vol. 91, pp. 1647–1651, May 2007.

[10] M. Zagrouba, A. Sellami, M. Bouaicha, and M. Ksouuri, "Identification of PV solar cells and modules parameters using the genetic algorithms: Application to maximum power extraction," *Sol. Energy*, vol. 84, pp. 860–866, 2010.

[11] H. Qin and J. W. Kimball, "Parameter determination of photovoltaic cells from field testing data using particle swarm optimization," in *Proc. Power Energy Conf. IL*, 2011, pp. 1–4.

[12] S. Liu and R. A. Dougal, "Dynamic multiphysics model for solar array," *IEEE Trans. Energy Convers.*, vol. 17, no. 2, pp. 285–294, Jun. 2002.

[13] A. N. Celik and N. Acikgoz, "Modeling and experimental verification of the operating current of mono-crystalline photovoltaic modules using four and five parameter models," *Appl. Energy*, vol. 84, pp. 1–15, 2007.

[14] R. Chenni, M. Makhlouf, T. Kerbache, and A. Bouzid, "A detailed modeling method for photovoltaic cells," *Energy*, vol. 32, pp. 1724–1730, 2007.

[15] O. Wasynczuk, "Modeling and dynamic performance of a line commutated photovoltaic inverter system," *IEEE Trans. Energy Convers.*, vol. 4, no. 3, pp. 337–343, Sep. 1989.

[16] M. AbdulHadi, A. M. Al-Ibrahim, and G. S. Virk, "Neuro-fuzzy-based solar cell model," *IEEE Trans. Energy Convers.*, vol. 19, no. 3, pp. 619–624, Sep. 2004.

[17] A. Chatterjee, A. Keyhani, and D. Kapoor, "Identification of photovoltaic source models," *IEEE Trans. Energy Convers.*, vol. 26, no. 3, pp. 883–889, Sep. 2011.

[18] J. P. Charles, I. M. Alaoui, G. Bordure, and P. Mialhe, "A critical study of the effectiveness of the single and double exponential models for I–V characterization of solar cells," *Solid-State Electron.*, vol. 28, no. 8, pp. 807–820, 1985.

[19] G. L. Araujo, E. Sanchez, and M. Martf, "Determination of the two-exponential solar cell equation parameters from empirical data," *Sol. Cells*, vol. 5, pp. 199–204, 1982.

[20] J. A. Gow and C. D. Manning, "Development of a photovoltaic array model for use in power electronics simulation studies," *IEE Proc., Electr. Power Appl.*, vol. 146, no. 2, pp. 193–200, Mar. 1999.

[21] A. Polman, W. G. J. H. M. V. Sark, W. Sinke, and W. Saris, "A new method for the evaluation of solar cell parameters," *Sol. Cells*, vol. 17, pp. 241–251, 1986.

[22] N. Enebish, D. Agchbayar, S. Dorjkhand, and D. Baatar, "Numerical analysis of solar cell current-voltage characteristics," *Sol. Energy Mater. Sol. Cells*, vol. 29, pp. 201–208, 1993.

[23] A. Hovinen, "Fitting of the solar cell iv-curve to the two diode model," *Physica Scripta*, vol. 54, no. T54, pp. 175–176, 1994.

[24] G. H. Yordanov, O. M. Midtgard, and T. O. Saetre, "Two-diode model revisited: parameters extraction from semi-log plots of i-v data," in *Proc. 25th Eur. Photovoltaic Sol. Energy Conf. Exhib.*, Valencia, Spain, Sep. 6–10, 2010, pp. 4156–4163.

[25] F. Adamo, F. Attivissimo, A. D. Nisio, and M. Spadavecchia, "Characterization and testing of a tool for photovoltaic panel modeling," *IEEE Trans. Instrum. Meas.*, vol. 60, no. 5, pp. 1613–1622, May 2011.

[26] J. A. Dolan, R. Lee, Y.-H. Yeh, C. Yeh, D. Y. Nguyen, S. Ben-Menahem, and A. K. Ishihara, "Neural network estimation of photovoltaic i-v curves under partially shaded conditions," in *Proc. Int. Joint Conf. Neural Netw.*, San Jose, CA, USA, 2011, pp. 1358–1365.

[27] F. Bryant and R. Glew, "Analysis of the current-voltage characteristics of cadmium sulphide solar cells under varying light intensities," *Energy Convers.*, vol. 14, no. 3–4, pp. 129–133, Jul. 1975.

[28] D. Sera, R. Teodorescu, and P. Rodriguez, "PV panel model based on datasheet values," in *Proc. IEEE Int. Symp. Ind. Electron.*, 2007, pp. 2392–2396.

[29] K. R. McIntosh, P. P. Altermatt, and G. Heiser, "Depletion-region recombination in silicon solar cells: When does $m_{DR} = 2$?," in *Proc. 16th Eur. Photovoltaic Sol. Energy Conf.*, 2000, pp. 251–254.

[30] J. Uspensky, *Theoty of Equations*. New York, NY, USA: McGRAW-Hill, 1948.

[31] N. Jacobson, *Basic Algebra*. San Francisco, CA, USA: W. H. Freeman, 1985.

[32] W. D. Soto, S. A. Klein, and W. A. Beckman, "Improvement and validation of a model for photovoltaic array performance," *Sol. Energy*, vol. 80, no. 1, pp. 78–88, Aug. 2006.

[33] M. Wolf, G. T. Noel, and R. J. Stirn, "Investigation of the double exponential in the current-voltage characteristics of silicon solar cells," *IEEE Trans. Electron Devices*, vol. ED-24, no. 4, pp. 419–428, Apr. 1977.

[34] Kyocera photovoltaic modules. [Online]. Available: http://www.kyocerasolar.com/pdf/specsheets/KC200GT.pdf

[35] "GEPV-110,110 watt photovoltaic module. [Online]. Available: http://www.powerupco.com/panels/ge/GEPV-110 Product Data Sheet.pdf

Authors' photographs and biographies not available at the time of publication.